Corrosion product transformations in alkaline baths under pressure and high temperature: The sub-critical stabilization of archaeological iron artefacts

M. Bayle[1,2], D. Neff[1], Ph. de Viviés[2], J-B. Memet[2], E. Foy[1], Ph. Dillmann[1]

[1] Laboratoire Archéomatériaux et Prévision de l'Altération, SIS2M/LAPA CEA Saclay

[2] A-CORROS Expertise, 23 Chemin des Moines, 13200 Arles, France

I- Introduction

The understanding of the corrosion processes of archaeological iron artefacts is of primary importance in the field of conservation. After centuries of burial or immersion in an archaeological site, iron artefacts are corroded and the nature of the corrosion products formed on the metallic surface is linked to the chemical conditions they have undergone. The alkalinity, the rate of oxygen and the presence of elements as chlorine or carbonate in the medium have a major influence on the crystallisation of the corrosion phases. For example in marine conditions, the high rates of chlorides and anoxic conditions lead to the formation of corrosion layers mainly composed of Fe(II) hydroxychloride $\beta\text{-}Fe_2(OH)_3Cl$. Another example is constituted of iron nails excavated from archaeological sites in calco-carbonic and anoxic solutions whose corrosion layers are constituted of iron carbonate (siderite $FeCO_3$ and chukanovite $Fe_2CO_3(OH)_2$), magnetite Fe_3O_4 and iron sulfide (greigite Fe_3S_4 and mackinawite), [1].

The excavation of century years old archaeological iron artefacts from the site creates a sudden disturbance of the environmental conditions mainly due to a massive flux of oxygen in the corrosion system. After excavation, the corrosion profile of the archaeological iron will evolve and phases can transform towards new phases. In some cases, this can cause severe degradation of the artefacts themselves or of the materials in contact with. The examples of the *Mary Rose* and the *Vasa* shipwrecks conservation show the issues of the evolution of an artefact after excavation in presence of iron sulphates and sulphides in the corrosion layers of the framework nails. The acidification conditions induced by the re-oxygenation of the corrosion products lead to the destruction of the organic artefact in contact with wood [2], [3]. Another crucial case concerns the artefacts immersed in marine environment. In this configuration the dissolution of the Fe(II) hydroxychloride is accelerate after excavation and can lead to the reactivation phenomenon of corrosion processes, damaging the metallic core initiating the breaking or transformation of the initial corrosion layer. This induces the recrystallization of iron Fe(III) oxyhydroxydes as goethite $\alpha\text{-}FeO(OH)$, lepidocrocite $\gamma\text{-}FeO(OH)$ and the chloride containing phase akaganeite $\beta\text{-}FeO_{1-x}(OH)_{1+x}Cl_x$ but also to oxides as magnetite Fe_3O_4 inside the transformed corrosion layer [4], [5], [6].

In order to avoid these degradations, to conserve properly the ferrous artefacts and to prepare the restoration work, prevention treatments are applied to stabilize them as soon as possible after excavation. In the case of artefacts from marine archaeological sites, several stabilization treatments are conducted and consist in extracting the chlorides from the corrosion layers. Alkaline baths in NaOH solutions are commonly applied on archaeological iron. Even these treatment proved to be efficient, their duration are very long, lasting in some cases several months to several years to extract the chlorides from the whole artefact. Over the last decade, in order to improve these stabilization treatments, the Clemson Conservation Center (Charleston, South Carolina, US) has developed a new process under sub-critical conditions [7]. It permits to reduce the duration from several weeks to only a few hours depending on the characteristics of the artefacts [8], [7], [9]. As for the treatment under ambient conditions, the artefact is immersed inside an alkaline bath and then the solution is pressurized around 35 bars and heated at 180°C (Fig 1a).

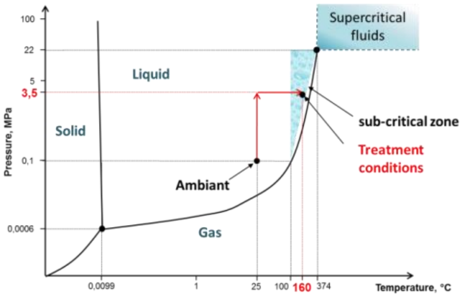

a)

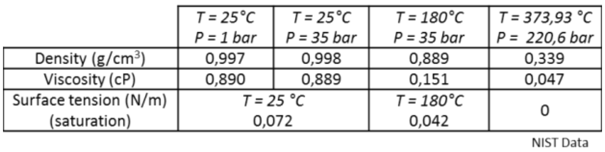

	T = 25°C *P = 1 bar*	*T = 25°C* *P = 35 bar*	*T = 180°C* *P = 35 bar*	*T = 373,93 °C* *P = 220,6 bar*
Density (g/cm^3)	0,997	0,998	0,889	0,339
Viscosity (cP)	0,890	0,889	0,151	0,047
Surface tension (N/m) (saturation)	*T = 25 °C* 0,072		*T = 180°C* 0,042	0

NIST Data

b)

Figure 1: a) Sub-critical working conditions on the pressure-temperature diagram of water. b) Values table of the water parameters in the treatment conditions [10].

Regarding former studies on stabilisation treatment at ambient conditions, the dechlorination process is based on the extraction of chloride thanks to dissolution of the chloride containing phases and to diffusion processes [4]. Working at higher pressure and temperature improve the transport properties. Figure 1.b shows that viscosity of water decreases from ambient conditions to the temperature of 180°C used during the treatment. We can expect that this behaviour will improve the wetting of the treated phases during the treatment but also the transport properties leading to reduce the duration of transformation mechanisms inside the corrosion layer of an iron artefact [10], [7].

Previous studies have compared the results of stabilisation obtained on archaeological artefacts through sub-critical techniques and traditional processes used for the dechlorination as alkaline bath with and without polarization (Fig. 2)

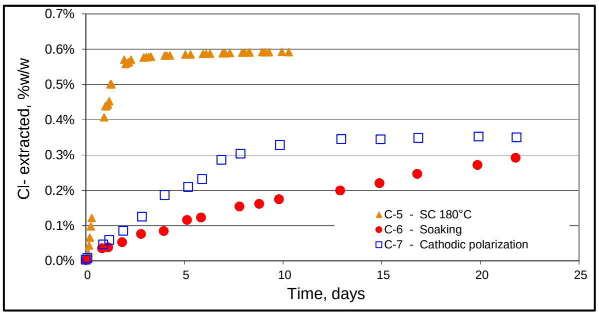

Figure 2: Comparison of the Cl- release rate during subcritical treatment of cast iron shell sections with 0.5w% NaOH at 180°C to the initial release rate from sections treated by soaking in 0.5w% NaOH and soaking with electrolysis at constant potential. Data from Clemson Conservation Center [11].

The Clemson Conservation Center compared the release of chlorides that occurred during subcritical dechlorination with soaking in a bath at ambient conditions and soaking under polarization of the treated artefact in alkaline bath. It is clearly observed that the subcritical dechlorination is completed after only two days whereas the two classical techniques are still continuing after more than 20 days. This comparison illustrates the efficiency of the technique for the dechlorination process. It has proven that the dechlorination is faster in sub-critical conditions and that it was complete after several days of treatment without disturbing the artefact general structure. Drews et al. treated many high purity iron oxides in subcritical conditions (180°C – 52 bars) and analysed them with Mossbauer spectroscopy and micro-raman spectroscopy after the treatments. The results show that akaganeite and lepidocrocite were transformed in a mixture of goethite and hematite. Goethite remained at 95% goethite and formed 5% of hematite. Magnetite partially transformed into hematite (22%) and no change was observed on pure hematite and maghemite [12]. But, even if observations of phases' transformation that occurred inside the corrosion layers during the process have been highlighted, mechanisms of transformation in these conditions are still unknown and the new phases obtained after complete dechlorination have not been sufficiently identified in order to determine the chemical pathways setting during the treatment.

Furthermore the formation of magnetite and hematite in low supercritical conditions has been studied by many authors especially along the coexistence curve between the boiling point and the critical point of water. Cook et al. established Pourbaix diagrams of the iron-water system between 300°C and 400°C and observed that increasing the temperature under the critical point in alkaline pH improve the crystallization of magnetite and hematite [13]. Davidson et al. performed in-situ XRD experiment in alkaline solution to follow the transformation of Schwertmannite ($Fe_8O_8(OH)_6SO_4$) which has a crystalline tunnel structure similar to akaganeite between 60°C and 240°C. The experiment evidenced that first the schwertmannite is transformed into ferrihydrite nanoparticles and then that two mechanisms can be observed. The first one shows that goethite is an intermediate product in the transformation to hematite and that temperature controlled this phenomenon. Above 200°C only hematite was obtained at the end of the transformation. The second mechanism shows the direct transformation of schwertmannite into hematite by diffusion processes [14].

The work presented here established the first observations that will lead to the understanding of the transformation phenomenon of archaeological or similar corrosion phases. The final aim is to improve the sub-critical process applied in the field of the conservation of historical artefacts. We would like to understand the transformation of the corrosion profile of archaeological iron artefacts during the subcritical stabilization from a macroscopic point of view to the microstructural scale in corrosion layers that proved to be heterogeneous at this scale. The objectives are to establish the physical and chemical mechanisms of the corrosion phases' transformation. For that, we worked on two directions. First we choose representative synthetic phases observed in corrosion profiles of archaeological iron. The characterizations were done before and after treatment in order to study their independent behaviour in sub-critical alkaline conditions. The second part of the study is focused on the profile transformation inside the corrosion layers of archaeological artefacts during the sub-critical stabilization. For that we selected a subaquatic profile obtained on iron framework nails from Arles Rhône 3 in order to perform first transformation tests on a real corrosion system.

II- Experimental

1/ Set of sample:

Synthetic phases

The first part is dedicated to the study of a selection of several phases commonly found on archaeological iron profiles excavated from many burial environments [15]. These phases are presented in table 1.

Table 1: Selected iron based phases studied in sub-critical conditions

Phases	Formula
Goethite	α-FeOOH
Akaganeite	$\beta\text{-FeO}_{1\text{-}x}(\text{OH})_{1+x}\text{Cl}_x$
Lepidocrocite	γ-FeOOH
Magnetite	Fe_3O_4
Maghemite	$\gamma\text{-Fe}_2\text{O}_3$
Hematite	$\alpha\text{-Fe}_2\text{O}_3$

First the work is focused on synthetic phases to understand their independent behaviour during 3 h sub-critical stabilization. For that, the samples were pressed into 5 mm pellets and placed in the reactor.

In the case of the study of the chlorinated Fe(III) oxyhydroxyde akaganeite, powders were synthetized at the laboratory following the Schwertmann synthesis' protocol [16]. It consists in heating a solution of 8.3g $FeCl_3$ $6H_2O$ in 500mL DIW during 48h at 70°C and then centrifuging and drying it at 70°C. In order to compare the behaviour of freshly synthetic phases to natural one, archaeological akaganeite was sampled on Istres Ingots from the 1st century and treated with the same conditions.

Archaeological iron nails

The archaeological artefacts selected for this study are iron nails excavated from the Arles Rhône 3 Roman barge from the 1st century. Their corrosion environment was a subaquatic and anoxic media and they were removed from the wood before their analysis on cross-sections. For that, the samples were mounted in epoxy resin and prepared by grinding (SiC, grade 180-4000) and polishing (diamond paste, 3 µm and 1 µm) under ethanol to avoid the phases' modification in contact with water. It has been verified that the corrosion profile are very similar on several nails. Considering that they are equivalent, part of the nails was observed before a subcritical process. Others were treated in the subcritical chamber during 5 h. All the nails were analysed following the same analytical protocol described below in order to determine the chemical and structural transformations of the corrosion profiles.

2/ Treatment protocol: The sub-critical A-CORROS© prototype

The study is followed in the A-CORROS© sub-critical chamber. The treatment consists in placing the samples in the 2 L chamber and to circulate a NaOH 0.125M solution continuously. The system is pressurized at 35 bars and then heated from 70°C to 180°C. The duration of treatment has been established to obtain the most representative results on samples in accordance with the experimental setup. The warming of the prototype was completed after 1h30 and the cooling were done in 1h. After the treatment, the samples were rinsed with deionised water to remove the residual solution and then dried at 60°C.

3/ Analytical protocol

In order to perform the characterisations both on synthetic phases and on archaeological artefacts, several techniques were used as optical microscopy, Raman spectroscopy, µXRD and SEM-EDS.

Raman spectroscopy was performed using a Renishaw InVia spectrometer. A frequency doubled Nd:YAG laser at 532 nm filtered to deliver 0.4 mW maximum was used to perform the analyses in order to avoid transformation due to local heating of the analysed material. The focus was adjusted with a microscope Leica LM/DM under the x50 objective. The analysed surface corresponds to a laser beam around 3 µm diameter. The spectra obtained with Raman spectroscopy were compared with former studies on similar materials [17], [18]. The XRD analyses were performed with a rotating anode source. The X-ray are delivered by a Molybdenum source at $E_{K\alpha}$ = 17,480 keV. The microscopic observations are done on a MEB-FEG (JEOL JSM-7001F, accelerating voltage of 15 kV) coupled with EDS analysis (SAMx IDFix software).

III- Results and discussion

Synthetic phases

The synthetic pellets phases treated in the subcritical reactor were analysed by Raman spectroscopy on their surface and a global analysis was performed with XRD. The results are summarised in the following table.

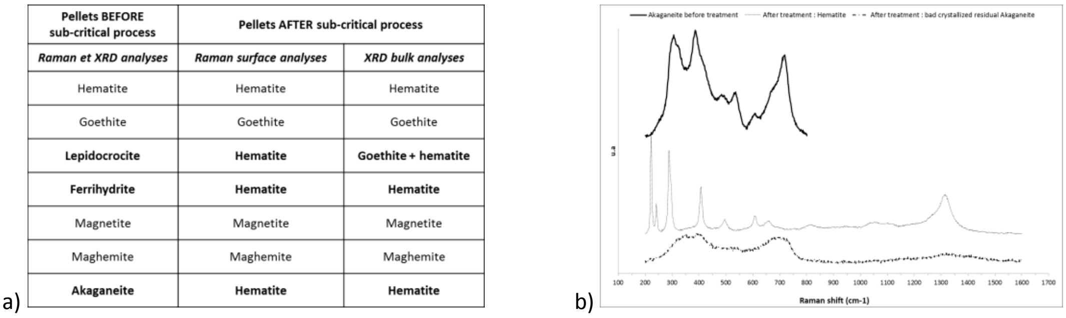

Pellets BEFORE sub-critical process	Pellets AFTER sub-critical process	
Raman et XRD analyses	*Raman surface analyses*	*XRD bulk analyses*
Hematite	Hematite	Hematite
Goethite	Goethite	Goethite
Lepidocrocite	**Hematite**	**Goethite + hematite**
Ferrihydrite	**Hematite**	**Hematite**
Magnetite	Magnetite	Magnetite
Maghemite	Maghemite	Maghemite
Akaganeite	**Hematite**	**Hematite**

Figure 3: a) Summary results obtained on synthetic phases before and after treatment characterizations with Raman spectroscopy and XRD. b) Synthetic akaganeite before and after treatment, Raman spectra.

As observed by Drews et al. [12] the principal phases obtained after treatments are hematite, magnetite and goethite (Fig 3a). As expected, hematite and magnetite didn't transform. Goethite remains goethite as well as maghemite. The synthetic chloride containing oxyhydroxyde akaganeite is transformed into hematite. The Raman analyses on figure 3b obtained on the surface of the pellet treated in sub-critical conditions show that the hematite signal obtained after treatment is well defined with the presence of characteristic peaks at 225 cm^{-1}, 245 cm^{-1}, 290 cm^{-1} and 415 cm^{-1}. Poorly crystallized residual akaganeite is also obtained from Raman spectroscopy.

SEM observations of synthetic akaganeite before the treatment show the presence of regular 0.5 µm long sticks (Fig 4a). After the subcritical process the crystals are completely transformed and irregular and large (around 1 µm diameter) hematite crystals were detected (Fig 4b). Before the sub-critical process, the synthetic akaganeite had a rate of 10%w of chlorines, measured by EDS analysis. After the transformation 1%w of chlorines was detected on the pellet. That rate corresponds to the local residual akaganeite of the pellet and no chlorine was detected on hematite crystals.

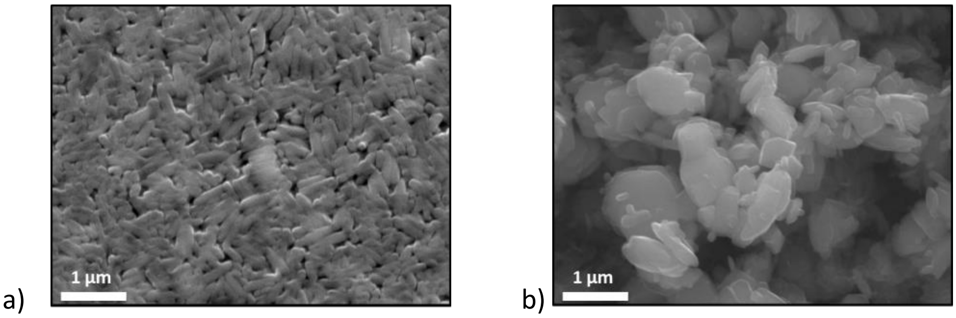

Figure 4: SEM observations (SE) of SYNTHETIC akaganeite before and after the sub-critical alkaline bath.

In order to study a phase more representative of archaeological corrosion products formed in-situ, the treatment was applied to an archaeological akaganeite sampled on Ingots from the 1st century corroded in marine environment and stored during 50 years at room conditions. The same experimental set-up (5 h at 180°C and 35 bars) than on synthetic akaganeite was used. Bulk analyses with XRD show the presence of akaganeite after the sub-critical process (fig. 5).

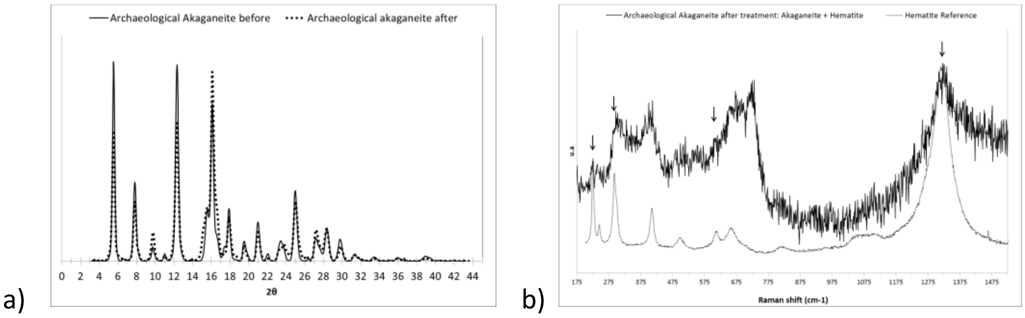

Figure 5: a) XRD bulk characterization of archaeological akaganeite before and after subcritical treatment. b) Raman spectroscopy analyses on the surface of the pellets before and after the sub critical treatment.

Hematite was not characterized with the bulk XRD analyses but Raman spectroscopy allows identifying the presence of both akaganeite and poorly crystallized hematite at the microscopic scale. SEM observations performed on the archaeological akaganeite before process show crystals of 1 µm long rod (Fig. 6a) whereas after the treatment we still observe the akaganeite crystals and also the presence of smaller and circular particles less than 0.3 µm identified as hematite via Raman spectroscopy analyses.

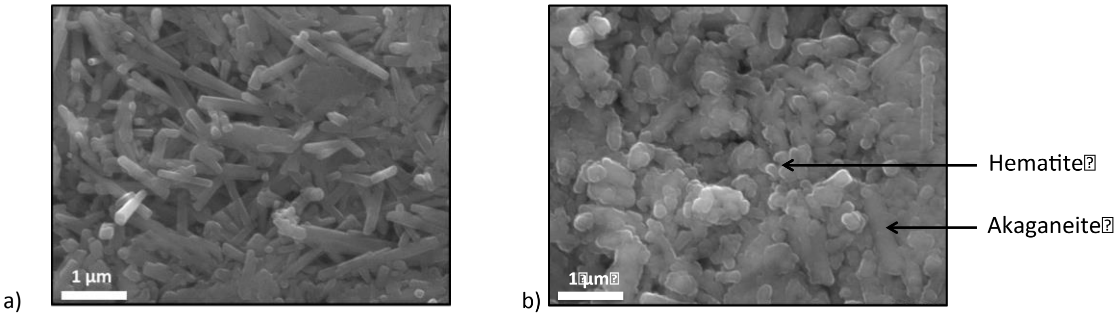

Figure 6: SEM images (SE) of ARCHAEOLOGICAL akaganeite a) before and b) after treatment in sub-critical alkaline solution.

EDS measurements show that sampled archaeological akaganeite contents 12w% of chlorines and that only 2%w of chlorines remain in the archaeological sample after this experimental set-up. This observation shows that the sample dechlorination is nearly completed after only 5 h of sub-critical process.

After the process, hematite was detected on both synthetic and archaeological samples. Working on synthetic phases give first and fast results considering the transformation products but archaeological samples permit to consider the real behaviour of corrosion phases in the field of conservation.

Archaeological artefacts

This first study on archaeological artefacts was done on samples from sub-aquatic and anoxic media in contact with wood. First the corrosion profile of the artefact through cross-sections observations and analyses directly after the excavation was determined. Then, the artefact was immersed in the reactor (NaOH 0.125 mol.L^{-1}), heated at 180°C and treated under 35 bars of pressure during 5 h. After the treatment the iron nails were rinsed with DIW and dried at 70°C. The same analyses were also performed on cross-sections prepared from treated samples.

From a macroscopic point of view, the artefacts were not disturbed by the treatment. No physical change was observed on the corrosion surface but the surface colour has changed from grey-green to black (Fig. 7a).

The figure 7b shows the corrosion profile of archaeological nails before the treatment. The presence of iron carbonates as chukanovite and siderite but also iron oxides as magnetite was identified on the profile by Raman spectroscopy. Moreover iron sulphides were detected at the extreme surface of the samples with the presence of a large majority of pyrite, FeS_2.

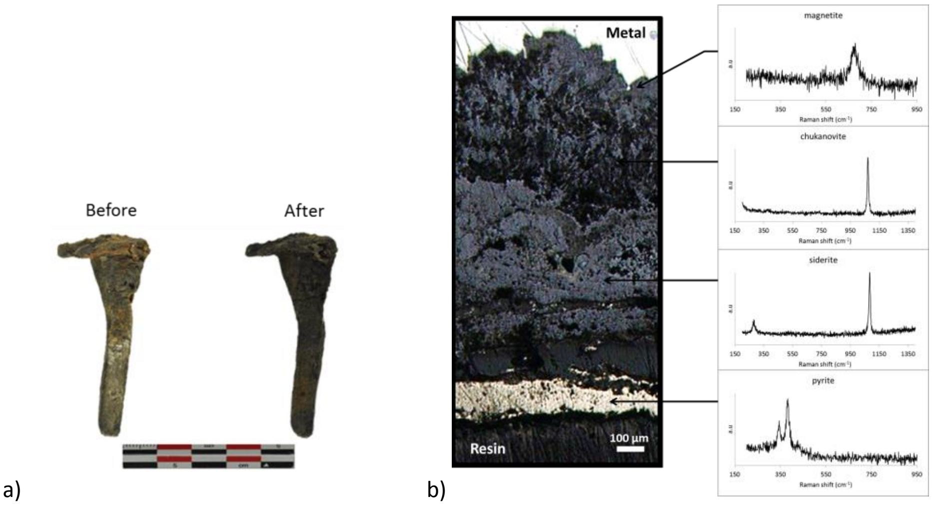

a) b)

Figure 7: a) Archaeological iron nails from Arles Rhône 3 before and after Sub-critical stabilization. b) Corrosion profile of archaeological iron nails before sub-critical treatment observed with optical microscopy and analysed with raman spectroscopy.

Under these specific conditions, the corrosion profile was not completely transformed through the stabilization. Local zones of several tenth micrometres still present iron carbonates as siderite and chukanovite in contact with the metallic core. The transformation product found in the more external part of the corrosion layers was magnetite, Fe_3O_4. The following SEM observation shows the transformation front inside the corrosion profile (Fig 8).

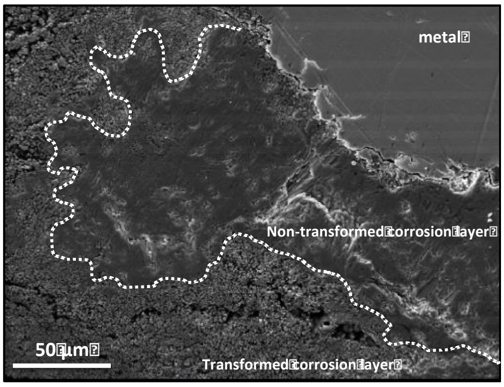

Figure 8: SEM image (SE) of the corrosion products along the metal core on cross-section.

The subcritical treatment applied on this archaeological artefact is not complete. The presence of magnetite inside the re-precipitated corrosion layers shows the impact of the subcritical alkaline solution on the chemical and physical transformation of the initial corrosion profile. No iron sulphide was found after the treatment. That observation allows to consider the use of sub-critical treatment for the stabilization of iron sulfides containing archaeological artefacts in the aim to avoid future destructive transformations of the corrosion products in contact with other types of materials during the storage.

IV- Conclusion

The sub-critical stabilization of archaeological artefacts has been studied in the field of the conservation of our metallic heritage. The efficiency of the technique in the way of the dechlorination of the corrosion layers of iron-based artefacts has been clearly proven.

The aim of the present study is to determine the transformations that occur inside the corrosion layers from the macroscopic to the microscopic scales. The first results obtained on synthetic phases allow focusing the study on the transformation phases obtained through the subcritical stabilization. Hematite and magnetite crystallization at these conditions must be better understood to improve the stabilization process of archaeological iron artefacts.

It is necessary to conduct further analyses to determine the impact of the fluid parameters on the nucleation and growth of transformation products during the subcritical stabilization. Moreover, the inherent parameters of the samples as the crystal size and the composition as the chloride rate in the case of akaganeite can have a relevant influence on the transformations mechanisms. That observation highlights the questions about the dechlorination phenomenon that occurred in archaeological iron artefacts. Indeed, it is difficult to say at this stage of the study whether the chlorides inside the akaganeite channels are evacuated before the structural transformation or if the two mechanisms are occurring at the same time.

The experimental set-up on archaeological artefact in sub-critical conditions presented in this study was performed during 5 hours and was not completed. This treatment seems to show that the phases' transformation is progressive and didn't disturb the corrosion layers distribution. In the aim of the conservation of archaeological artefacts and in order to perform restorations, it is important to conserve the historical information contained in the corrosion layers. We can expect that for a longer treatment, the corrosion layer morphology will evolve and that the impact of the time parameter must be understood properly to optimize the stabilization process. The crystals nucleation and growth will be controlled to obtain resistant and stable corrosion layers of archaeological artefacts.

V- Acknowledgements

The authors would like to acknowledge Solenn Reguer for her relevant help during the project and the several experiments and Jean-Louis Hazemann for his help in the experiment development in subcritical conditions and for the several exchanges on the subject.

VI- References

1. Saheb, M., et al., *Long-term corrosion behaviour of low-carbon steel in anoxic environment: Characterisation of archaeological artefacts.* Journal of Nuclear Materials, 2008. **379**(1-3): p. 118-123.
2. Schofield, E.J., et al., *Nanoparticle de-acidification of the Mary Rose.* Materials Today, 2011. **14**(7-8): p. 354-358.
3. Fors, Y., et al., *Sulfur accumulation in pinewood (Pinus sylvestris) induced by bacteria in a simulated seabed environment: Implications for marine archaeological wood and fossil fuels.* International Biodeterioration & Biodegradation, 2008. **62**(4): p. 336-347.
4. Kergourlay, F., *Etude des mécanismes de déchloruration d'objets archéologiques ferreux corrodés en milieu marin. Cas des traitements en solutions alcalines aérée et désaérée.* 2012, Créteil Paris-Est: Paris. p. 262.
5. Reguer, S., P. Dillmann, and F. Mirambet, *Buried iron archaeological artefacts: Corrosion mechanisms related to the presence of Cl-containing phases.* Corrosion Science, 2007. **49**(6): p. 2726-2744.
6. Reguer, S., *Phases chlorées sur les objets archéologiques ferreux corrodés dans les sols : caracterisation et mecanismes de formation*. 2005, université Paris sud, XI. p. 330.
7. Gonzalez, N., et al., *The use of subcritical fluids for the stabilization of concreted iron artefacts*, in *METAL 2010 Interim meeting of the ICOM-CC Working Group*, P. Mardikian, et al., Editors. 2010: Charleston. p. 39-53.
8. Näsänen, L.M.E., et al., *The applicability of subcritical fluids to the conservation of actively corroding iron artifacts of cultural significance.* The journal of supercritical fluids, 2013. **79**: p. 289-298.
9. Gonzalez, N., et al., *The effects of cathodic polarization, soaking in alkaline solutions and subcritical water on cast iron corrosion products*, in *METAL 07 Interim meeting of the ICOM-CC Metal Working Group*, C. Degrigny, et al., Editors. 2007: Amsterdam. p. 32-37.
10. NIST, *NIST Chemistry WebBook NIST Standard Reference Database*, Linstrom, P. J. Mallard, W. G.: Gaitherburg MD, http://webbook.nist.gov
11. Drews, M., et al., *The application of subcritical fluids for the stabilization of marine archaeological iron.* Studies in Conservation, 2013. **58**(4): p. 314-325.
12. Drews, M., N.G. Gonzalez-Pereyra, and D. Cook. *The transformation of iron oxides, oxyhydroxides and corrosion products by subcritical water treatment*. in *Interim meeting of the ICOM-CC Metal working group*. 2013. Edinburgh.
13. Cook, W.G. and R.P. Olive, *Pourbaix diagrams for the iron-water system extended to high-subcritical and low-supercritical conditions.* Corrosion Science, 2012. **55**: p. 326-331.
14. Davidson, L.E., S. Shaw, and L.G. Benning, *The kinetics and mechanisms of swertmannite transformation to goethite and hematite under alkaline conditions.* American Mineralogist, 2008. **93**: p. 1326-1337.
15. Neff, D., et al., *A review of the archaeological analogue approaches to predict the long-term corrosion behaviour of carbon steel overpack and reinforced concrete structures in the French disposal systems.* Journal of Nuclear Materials, 2010. **402**(2-3): p. 196-205.

16. Cornell, R. and U. Schwertmann, *The iron oxides - Structure, Properties, Occurences and Uses*. 2nd edition ed. 2003, Weinheim: Wiley-VCH Verlag.
17. Neff, D., et al., *Structural characterization of corrosion products on archaeological iron: an integrated analatycal approach to establish corrosion forms.* Journal of Raman Spectroscopy, 2004. **35**: p. 739-745.
18. Bouchar, M., et al., *The complex corrosion system of a medieval iron rebar from the Bourges'Cathedral. Characterization and reactivity studies.* Corrosion Science, 2013. **76**: p. 361-372.